Theory of eccentric photorefraction (photoretinoscopy): astigmatic eyes

Wolfgang Wesemann

Höhere Fachschule für Augenoptik Köln, Bayenthalguertel 6-8, 5000 Cologne-51, Germany

Anthony M. Norcia

The Smith-Kettlewell Eye Research Institute, 2232 Webster Street, San Francisco, California 94115

Dale Allen

College of Optometry, University of Houston, Houston, Texas 77004

Received June 24, 1991; accepted July 3, 1991

An optical analysis of eccentric photorefraction (photoretinoscopy) of astigmatic eyes is presented. The size and the angular tilt of the dark crescent appearing in the subject's pupil are derived as a function of five variables: the ametropia of the eye (D_{sph}, D_{cyl}, axis), the eccentricity of the flash, e, and the distance of the camera from the subject's eye, d_c. A simplified solution and a solution of the inverse problem, which enable one to calculate the degree of ametropia from the size and the tilt of the crescent, are also presented. If the crescent is smaller than the pupil, both the size and the tilt of the dark crescent are independent of the pupil size. The angular tilt of the crescent is also independent of the eccentricity. Characteristic changes of the crescent as a function of the cylinder axis are illustrated for compound and mixed astigmatisms. The validity of the theoretical predictions was experimentally verified on a model eye.

1. INTRODUCTION

Eccentric photorefraction, also termed photoretinoscopy, is an objective method for estimating ametropia that bears many similarities to retinoscopy and to the working principle of contemporary automated eye refractors. In retinoscopy the examiner observes the movements of a crescent-shaped light reflex appearing in the pupil. Depending on the direction of motion of the reflex, the examiner adds plus or minus lenses to find the neutral point. The automatic eye refractor manufactured by Humphrey Instruments utilizes stationary light sources situated immediately adjacent to the optical axis. A four-quadrant detector positioned at the optical axis determines in which part of the pupil a crescent appears. The position of the crescent is used to control a Badal optometer and a set of variable Stokes cylinder lenses to compensate for the ametropia.

In contrast to these two compensation (nulling) techniques, photoretinoscopes are used to estimate the magnitude of the ametropia from the absolute size and shape of the light reflex in the pupil. Since no attempt is made to neutralize the ametropia, this method may never yield the accuracy of retinoscopy.[1] However, it has the unique advantage that the ametropia of both eyes can be determined at the same time, thus guaranteeing equal states of accommodation. This advantage is especially important for infants or young children without cycloplegia.

After the publication of the research of Howland and Howland[2] and Howland *et al.*[3] on the isotropic photorefractor, in which the observation and the illumination paths are coaxial, several different devices appeared that incorporated an eccentrically mounted light source. Kaakinen[4-6] constructed a photorefractor by placing an electronic flash unit just outside the entrance pupil of a 100-mm objective attached to a 35-mm still camera. Hay *et al.*[7] employed a 1000-mm catadioptric lens and an electronic flash. A similar method was subsequently used by Day and Norcia[8] and Norcia *et al.*[9] Molteno *et al.*[10] designed a photographic objective in which the first component of the lens formed the limiting aperture of the system, around which was placed an annular flash. Bobier and Braddick[11] placed a fiber-optic bundle near the entrance pupil of a $f/2.5$ 105-mm lens attached to a video camera. Schaeffel *et al.*[12] and Angi and Cocchiglia[13] presented infrared photoretinoscopes that use high-output light-emitting diodes in combination with a video camera. This technique has been fruitfully applied for the study of the development of myopia (Schaeffel and Howland[14]).

A number of different names have been suggested for these photographic refraction techniques based on Foucault's knife-edge test[15]: static photoskiascopy,[16] eccentric photorefraction,[11] paraxial photorefraction,[17] and photoretinoscopy.[12,18]

Several ray-tracing analyses of knife-edge photorefractors have appeared.[11,18] However, these analyses are restricted to special cases, namely, a spherical ametropia, or an astigmatic error, with its main meridian either parallel or perpendicular to the camera–flash axis. These analyses cannot explain the behavior of the crescent in an astigmatic eye with an oblique axis because such a refractive error gives rise to an oblique, tilted crescent. The

0740-3232/91/122038-10$05.00

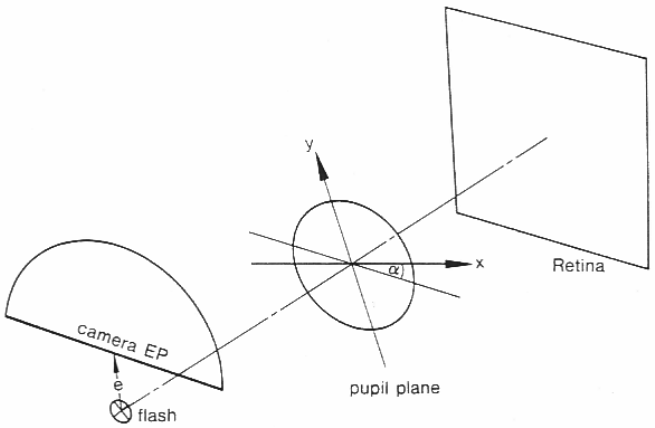

Fig. 1. Photorefractor with a light source mounted at an eccentricity e below the entrance pupil (EP) of the camera. The diagram denotes the rotating x–y coordinate system used in Appendix A.

analytic derivation presented below is a solution for the general case and enables one to explain the behavior of the crescent for all forms of refractive error.

2. BASIC PREMISE

We consider a photorefractor as illustrated in Fig. 1. The border of the entrance pupil (EP) of the camera adjacent to the flash is assumed to be a straight horizontal line at an eccentricity e above the flash. We sometimes refer to the straight horizontal border as knife edge. The flash is assumed to be a point source located on the optical axis. This geometry closely resembles the infrared photoretinoscope of Schaeffel *et al.*[12] but differs from the design of other existing photorefractors. These existing photorefractors use not a straight border but the circular edge of the camera aperture as the occluding edge.

The derivation makes use of the following approximations:

(1) The optical system of the eye is approximated by a thin lens.

(2) Spherical aberration and other optical errors are neglected.

(3) For convenience, the eye is considered an air–air system, so that the object and the image focal lengths are equal.

(4) The diameter of the EP of the camera is assumed to be large.

3. SPHERICAL AMETROPIA

The image-forming geometry of a knife-edge photorefractor is plotted in Fig. 2 for a myopic eye. A similar, but slightly incorrect, diagram has already been published.[19]

The size of the dark crescent, *DCR*, in the pupil of a rotationally symmetric eye can be derived from Fig. 2 by an elementary analysis of similar triangles (see also Bobier and Braddick[11]). The size of the dark crescent is

$$DCR = e/(d_c D_{\text{sph}} - 1), \tag{1}$$

where e denotes the eccentricity of the flash. D_{sph} is the refractive power of the lens that would be required to correct the eye's spherical ametropia (myopia requires a negative lens). The distance of the camera from the subject's eye, d_c, is negative because it is measured against the conventional direction of light propagation. *DCR* is positive when the eye is myopic relative to the camera distance. The positive sign indicates that the dark portion of the crescent appears on the side of the camera lens (in the upper part of the pupil for the arrangement indicated in Figs. 1 and 2). *DCR* is negative in the case of a hyperopic eye, indicating that the dark crescent appears on the side of the flash.

When the photoretinoscope is used to determine the refractive state of an eye having an astigmatism with or against the rule (cylinder axis $\alpha = 0°$ or $\alpha = 90°$ in minus-cylinder form), the crescent size can be obtained from a modified Eq. (1) because the horizontally aligned refractor is sensitive to the ametropia only in the vertical main meridian of the eye.

In the case of an astigmatism with the rule, the vertical meridian is the principal meridian with the greater refractive power. This meridian is corrected by a lens with power $D_{\text{sph}} + D_{\text{cyl}}$, where D_{cyl} denotes the magnitude of the correcting minus cylinder, and the dark crescent size *DCR1* is given by

$$DCR1 = e/[d_c(D_{\text{sph}} + D_{\text{cyl}}) - 1]. \tag{2}$$

Given an astigmatism against the rule, the dark crescent size *DCR2* is

$$DCR2 = e/(d_c D_{\text{sph}} - 1). \tag{3}$$

In these special cases the border of the crescent is perpendicular to the line connecting the centers of the flash and the camera lens.

Note that the size of the dark crescent is independent of the pupil size. Thus the pupil size can be omitted in the algebraic formulation of the problem. However, pupil size is not irrelevant. In practice, it is normally easier to measure the size of the bright crescent. Furthermore, pupil size is an important constraint on the sensitivity and the accuracy of the method (see Section 8).

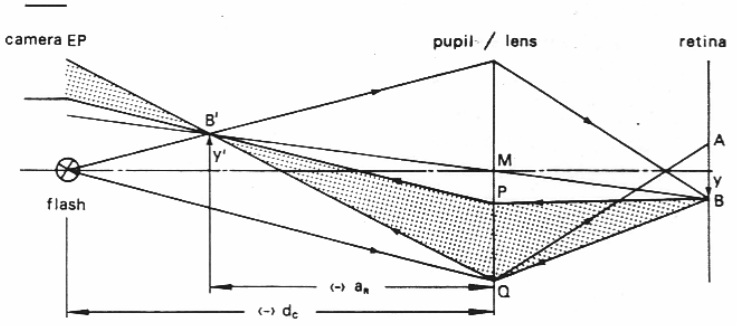

Fig. 2. Crescent formation with a myopically defocused eye. A flash source is positioned on the optical axis at a distance $(-)d_c$ in front of the eye. The eye is myopically focused with respect to the flash. The flash is imaged to a point in front of the retina and generates a blur circle with diameter AB on the retina. The lower boundary point of the blur circle B is imaged to a corresponding point B′ in the far point plane outside the eye. Of all rays passing through B and B′, only those inside the dotted area can enter the entrance pupil of the camera. They create a bright crescent of size PQ in the lower part of the pupil.

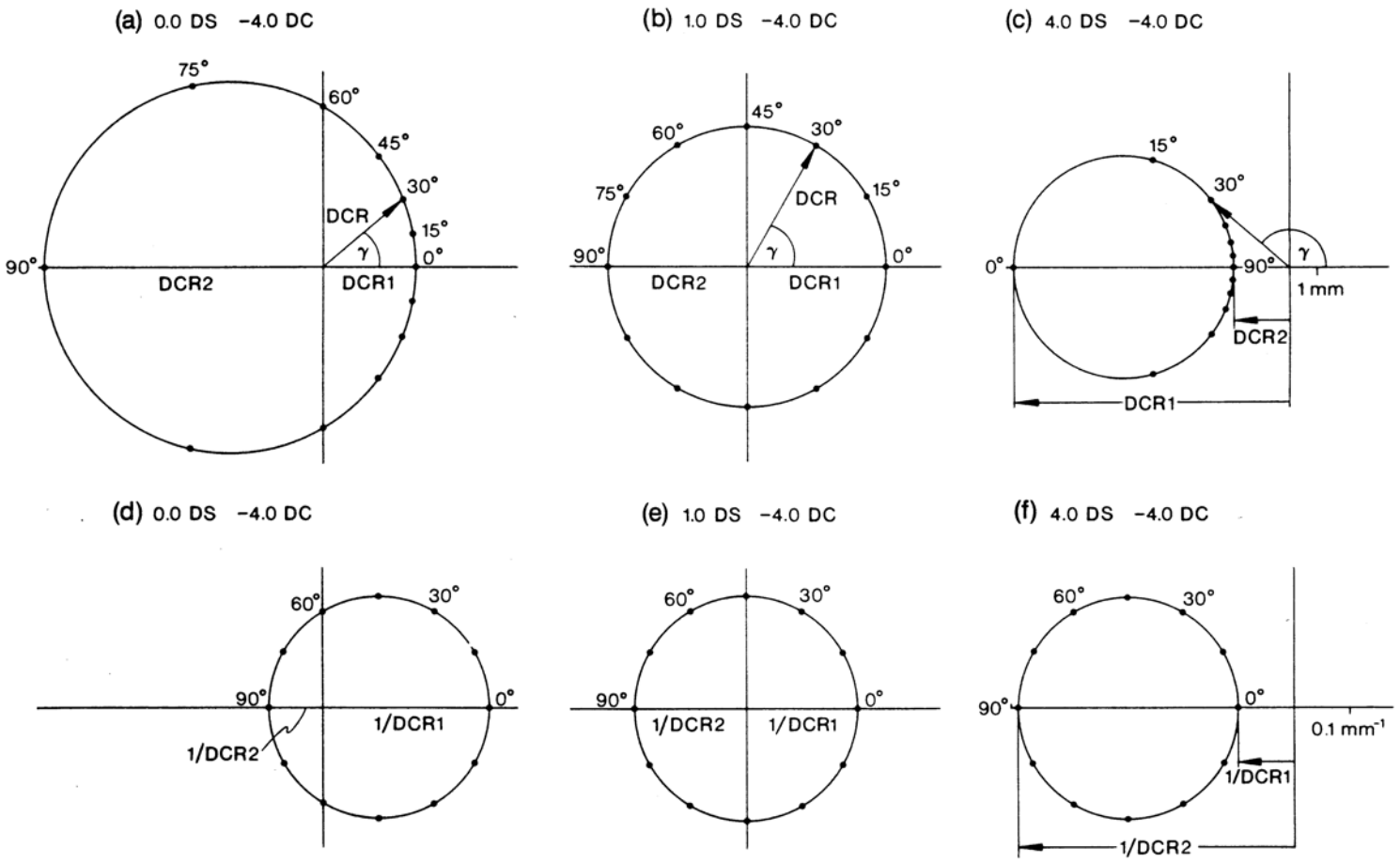

Fig. 3. (a)–(c) Polar diagrams of the crescent vector (DCR,γ) for three astigmatic ametropias and parametrically varied cylinder axis. The size of the dark crescent is indicated by the distance of the circumference of the circle from the origin. The numbers on the circumference of the circle denote the cylinder axis α. The arrows indicate the dark crescent for a cylinder axis of 30°. For the special case of an astigmatism with or against the rule ($\alpha = 0°$ or $\alpha = 90°$), a horizontal border of the crescent is obtained ($\gamma = 0°$ or $\gamma = 180°$). In this case the dark crescent size is *DCR1* or *DCR2* as defined in Eqs. (2) and (3), respectively. The question of whether the crescent will be visible can be answered by drawing a circle with a radius equal to the pupil diameter around the origin [see the scale in (c)]. Only those conditions that generate a crescent vector that lies inside the pupil will create a visible crescent. (d)–(f) Polar diagrams of the transformed crescent vector $(1/DCR,\gamma)$. Ametropias are as in (a)–(c). The cylinder axis now varies in an orderly manner independent of ametropia.

4. RAY-TRACING APPROACH TO ASTIGMATIC EYES: NUMERICAL RESULTS

In the case of an oblique astigmatism the crescent is tilted, and the size of the dark crescent has an intermediate value between *DCR1* and *DCR2*.

With the rigorous analytic ray-tracing approach, described in Appendix A, we derive the size *DCR* and the tilt γ of the dark crescent as a function of six variables, namely, (1) the spherical and (2) the cylindrical powers of the corrective spectacle lens at vertex distance 0, D_{sph} and D_{cyl}; (3) the axis of the cylinder, α; (4) the eccentricity of the flash from the camera, e; (5) the radius of the pupil, R_p; and (6) the distance d_c of the camera from the subject's eye:

$$(DCR,\gamma) = f(D_{sph}, D_{cyl}, \alpha, e, R_p, d_c). \quad (4)$$

For each set of input data we obtain a pair of data forming a vector with magnitude *DCR* and phase angle γ. A convenient way to illustrate the behavior of the dark crescent is to draw the vector in a polar diagram for a given set of input data. This has been done in Figs. 3(a), 3(b), and 3(c) for a fixed camera distance of −1 m, an eccentricity of 10 mm, and ametropias of 0.0 DS, −4.0 DC; 1.0 DS, −4.0 DC; and 4.0 DS, −4.0 DC, respectively. In each panel the axis of the cylinder axis was varied parametrically from 0° to 180°.

The polar diagrams in Figs. 3(a)–3(c) show that the vector $(DCR,\ \gamma)$ approaches a perfect circle for a fixed refractive power and varying cylinder axis. The x coordinates at the right-hand and left-hand x intercepts of the circle, *DCR1* and *DCR2*, define the size of the crescent for an astigmatism with or against the rule. *DCR1* and *DCR2* are numerically equal to the results obtained with the basic Eqs. (2) and (3). A positive x intercept denotes that the respective principal meridian is myopic with respect to the camera; a negative x intercept is generated by a hyperopic principal meridian.

We can answer the question as to whether a crescent appears in the pupil from Figs. 3(a)–3(c) for any given pupil size simply by drawing a circle with a radius equal to the diameter of the pupil around the origin. All conditions that create a dark crescent vector $(DCR,\ \gamma)$ that lies fully inside the pupil circle will give rise to a visible crescent. All conditions generating a crescent vector that points to a locus outside the pupil circle show a totally dark pupil because the dark crescent size *DCR* is larger than the diameter of the pupil.

The circle described by the dark crescent vector is centered at the origin in the case of a symmetric mixed astigmatism [Fig. 3(b)]. This placement means that the size of the crescent does not change with varying cylinder axes. A crescent of constant size appears at all angles α and rotates along the rim of the pupil. [To avoid confu-

sion, we should note that the ametropia of 1.0 DS, −4.0 DC, assumed in Fig. 3(b), represents a symmetric mixed astigmatism with respect to the camera because the assumed distance of the camera (−1 m) is equivalent to a myopia of −1 DS. Thus the center of the dead zone of the photorefractor is located at −1 DS.]

The numbers at the circumference of the circle denote the values of the cylinder axis α. They enable one to compare the pace at which the tilt of the crescent changes. It is obvious that a simple relationship between the cylinder axis and the tilt of the crescent exists in symmetric mixed astigmatism [Fig. 3(b)]. In this case the tilt of the crescent is always equal to exactly twice the cylinder axis. In Fig. 3(a), which was calculated for an asymmetric mixed astigmatism, the tilt of the crescent rotates by a large amount (90°) when the cylinder axis α rotates from 90° to 60° and decelerates its rotational speed with decreasing cylinder angle.

In both Figs. 3(a) and 3(b) the crescent rotates through the full range of 360° when the cylinder axis varies from 0° to 180°. This means that the dark crescent is located in the upper part of the pupil at α = 0° and rotates counterclockwise along the rim of the pupil with increasing cylinder axis. This behavior is typical for a mixed astigmatism.

In a compound astigmatism [Fig. 3(c)] the tilt of the crescent γ is always smaller than 90° because the circle lies entirely on one side of the coordinate system. In the example in Fig. 3(c) the angle of the crescent deviates only by less than 45° from the horizontal axis and changes in a scissorlike movement against the rotating cylinder axis.

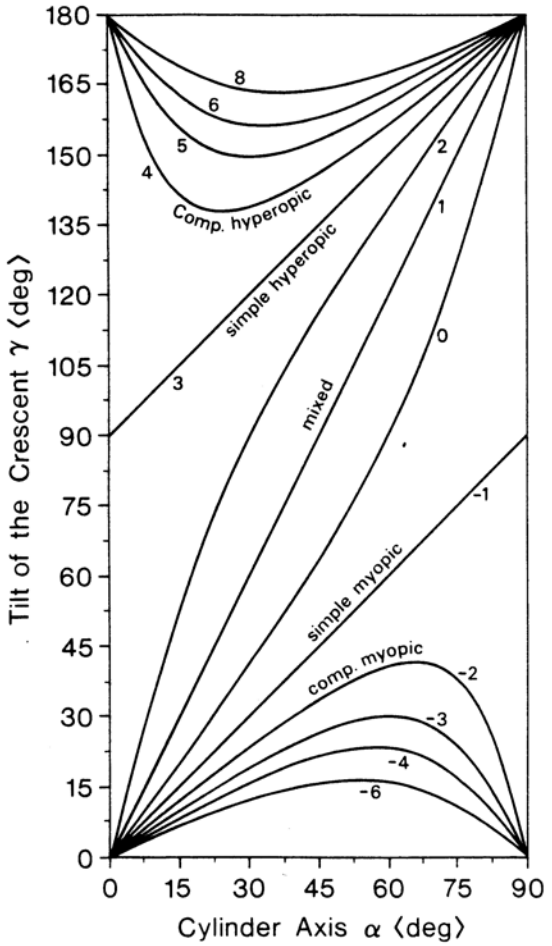

Fig. 4. Tilt of the crescent as a function of the cylinder axis. The spherical power of the corrective lens changes parametrically while the cylinder power is held constant at −4 D. The camera distance was assumed to be 1 m. An eye having an ametropia of −1 D would be in focus with respect to the camera plane. Thus an astigmatic ametropia of +1 DS, −4 DC, having a spherical equivalent of −1 DS, is a symmetric mixed astigmatism with respect to the camera distance. The behavior in five distinct regions is explained in the text.

Figure 4 summarizes further details of the behavior of the tilt for a number of astigmatic ametropias. The cylinder power was kept constant at −4 DC. The spherical power was varied parametrically from −6 to +8 DS. All curves are plotted as a function of the axis of the corrective minus cylinder. The graph is rotationally symmetric with respect to the point (α = 45°,γ = 90°).

Figure 4 shows five distinctly different regions:

(1) In the region of compound myopic astigmatisms, the tilt of the crescent is always smaller than the cylinder axis. When the cylinder axis is rotated through 90°, the tilt of the crescent initially follows the rotation but eventually falls back to 0° tilt.

(2) In the case of a simple myopic astigmatism, the tilt is always identical to the axis of the cylinder.

(3) In the region of mixed astigmatisms the crescent always rotates faster than the cylinder axis. When the cylinder axis is rotated through 90°, the tilt of the crescent rotates through a full 180°. In the case of a symmetric mixed astigmatism the crescent rotates at exactly twice the rate of the cylinder axis.

(4) The tilt is equal to 90° + α for a simple hyperopic astigmatism.

(5) The tilt is always larger than 90° + α in cases of compound hyperopic astigmatisms.

In the case of ametropia close to a simple astigmatism with respect to the camera distance, the tilt of the crescent can never be seen near the two discontinuities at (α = 0°,γ = 90°) and (α = 90°,γ = 90°), where the meridional refractive error is zero and the dark crescent size grows beyond all boundaries. The absence of the crescent could be mistaken as evidence for an emmetropic eye, but actually the dark pupil is simply a consequence of the absolute insensitivity of knife-edge photorefractors to refractive errors in the axis orthogonal to the camera–flash axis. The extent of this angular dead zone depends mainly on the eccentricity e, but it also depends on the linear dimensions of the flash tube and the size of the EP of the camera (see Section 8). It should be evaluated experimentally for the actual geometry of the photorefractor.

5. SIMPLIFIED FORWARD SOLUTION

From the behavior of the size and the tilt of the dark crescent described in Section 4, a simplified solution can be derived. As is shown in Figs. 3(a)–3(c), the polar diagram of the crescent approaches a perfect circle, with its x intercepts, *DCR1* and *DCR2*, being defined by the refractive powers in the two respective principal meridians. The starting point for the simplified solution is the fact that the polar diagram can be made symmetric with respect to the cylinder axis by the transform

$$r' = 1/DCR, \qquad \gamma' = \gamma. \tag{5}$$

This transformation replaces the size of the dark crescent by its inverse and leaves the angle of the crescent unaltered. The effect of this transformation is illustrated

in Figs. 3(d)–3(f). The transformed polar diagram ($1/DCR$, γ) is also a perfect circle, but now the cylinder axis α rotates always at a constant speed around the center of the circle. After elementary operations, the center of the transformed circle is found to be situated at

$$x_m' = \left(\frac{1}{DCR1} + \frac{1}{DCR2}\right) \Big/ 2 = \frac{d_c}{e}\left(D_{\text{sph}} + \frac{1}{2}D_{\text{cyl}} - \frac{1}{d_c}\right). \tag{6}$$

Thus the center of the transformed circle is located at a position proportional to the spherical equivalent, $D_{\text{sph}} + (1/2)D_{\text{cyl}}$, corrected for the distance of the camera $1/d_c$. The radius of the circle is

$$R' = \left(\frac{1}{DCR1} - \frac{1}{DCR2}\right) \Big/ 2 = \frac{d_c D_{\text{cyl}}}{2e}. \tag{7}$$

The radius of the circle in the transformed coordinate system is independent of the spherical power and proportional to the power of the cylinder.

Since the cylinder axis rotates at a constant speed, the transformed circle is completely described by its parametric form

$$x' = R' \cos(2\alpha) + x_m', \tag{8}$$

$$y' = R' \sin(2\alpha). \tag{9}$$

Now, it is possible to calculate the absolute value of the dark crescent DCR and the tilt γ of the crescent from

$$DCR = 1/(x'^2 + y'^2)^{1/2}, \tag{10}$$

$$\gamma = \arctan(y'/x'). \tag{11}$$

After inserting Eqs. (6)–(9) into Eqs. (10) and (11), we find, after elementary operations, the following general expressions for the size and the tilt of the dark crescent as a function of an arbitrary ametropia

$$|DCR| = \left(\frac{d_c^2}{e^2}\left\{\left(D_{\text{sph}} - \frac{1}{d_c}\right)^2 + D_{\text{cyl}}\left(D_{\text{sph}} + \frac{D_{\text{cyl}}}{2} - \frac{1}{d_c}\right) \times [1 + \cos(2\alpha)]\right\}\right)^{-1/2}, \tag{12}$$

$$\gamma = \arctan\left[\frac{D_{\text{cyl}} \sin(2\alpha)}{D_{\text{cyl}} \cos(2\alpha) + 2D_{\text{sph}} + D_{\text{cyl}} - 2/d_c}\right]. \tag{13}$$

The sign of the dark crescent size DRC is connected with the sign of the denominator in Eq. (13). Finally, DCR can be expressed as

$$DCR = \text{sgn}[D_{\text{cyl}} \cos(2\alpha) + 2D_{\text{sph}} + D_{\text{cyl}} - 2/d_c] * |DCR|, \tag{14}$$

where sgn represents the sign function.

These more intuitively derived formulas give numerical results that are in agreement with the rigorous ray-tracing approach described in Appendix A. In addition, Eq. (12) has the important property of being identical to the basic Eq. (1) when the cylinder power is set to 0.

6. THE INVERSE SOLUTION: DEGREE OF AMETROPIA CALCULATED FROM CRESCENT PARAMETERS

Equations (13) and (14) describe the size and the tilt of the crescent as a function of ametropia. The practitioner is naturally more interested in the inverse solution, i.e., the calculation of the degree of ametropia from the measured crescent size and tilt. Obviously, the three parameters that specify the ametropia (D_{sph}, D_{cyl}, α) cannot be derived from two equations. Thus at least two independent pictures of the crescent are required. We can achieve this requirement, e.g., by taking two pictures in two orthogonal orientations of the photorefractor.

We assume that the first picture is taken with a horizontally aligned photorefractor, as shown in Fig. 1, and the second with the photorefractor rotated by 90°. In the first picture, with normal orientation, the photorefractor sees the actual ametropia of D_{sph}, D_{cyl}, α. In the second picture it sees an ametropia of D_{sph}, D_{cyl}, $(\alpha + 90°)$. Assuming that crescents are visible in both pictures, we can specify the two observed crescents by their sizes, DCR_h and DCR_v, and tilts, γ_h and γ_v, respectively. By inserting these four values into Eqs. (12) and (13), we obtain four equations from which the unknown quantities D_{sph}, D_{cyl}, and α can be determined. After a number of elementary transformations, we finally obtain

$$D_{\text{cyl}} = -(2k_1 - 4k_3^2)^{1/2}, \tag{15}$$

$$D_{\text{sph}} = k_3 + \frac{1}{d_c} - \frac{1}{2}D_{\text{cyl}}, \tag{16}$$

$$\alpha = \text{sgn}(DCR_h) * \text{sgn}(\gamma_h) * (1/2)\arccos(k_2/k_4), \tag{17}$$

with the abbreviations

$$k_1 = \frac{e^2}{d_c^2}\left(\frac{1}{DCR_h} + \frac{1}{DCR_v}\right),$$

$$k_2 = \frac{e^2}{d_c^2}\left(\frac{1}{DCR_h} - \frac{1}{DCR_v}\right),$$

$$k_3 = \text{sgn } k_3 * \left\{\frac{k_2[\sin(\gamma_v - \gamma_h)]}{4[\sin(\gamma_v + \gamma_h)]}\right\},$$

$$k_4 = 2D_{\text{cyl}}\left(D_{\text{sph}} + \frac{1}{2}D_{\text{cyl}} - \frac{1}{d_c}\right).$$

One of the problems encountered in the course of the derivation is the fact that the important signs are lost when we take the square root. These signs had to be recovered afterward. For the sign of k_3, we adopted the sign rule

$$\text{sgn } k_3 = \begin{cases} -\text{sgn}(DCR_h) & \text{if } \text{sgn}(DCR_h) = \text{sgn}(DCR_v) \\ -\text{sgn}(DCR_h) * \text{sgn}[\sin(\gamma_v - \gamma_h)] * \text{sgn}(\gamma_h) & \text{if } \text{sgn}(DCR_h) \neq \text{sgn}(DCR_v). \end{cases}$$

A few comments are added concerning the applicability of the inverse solution:

(1) The size of the measured tilted crescents is negative when the larger part of the dark crescent lies on the side of the flash.

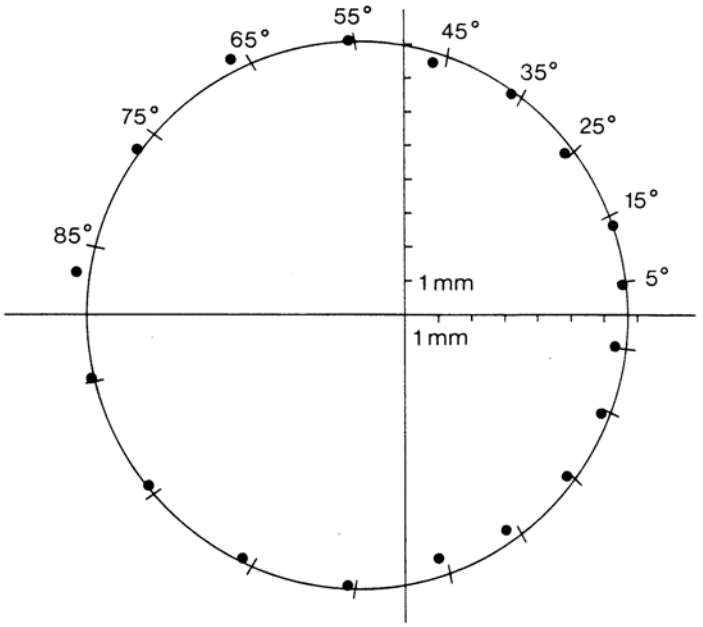

Fig. 5. Polar diagram of the crescent vector predicted by Eqs. (13) and (14) for an astigmatic ametropia of 0.25 DS, −3.0 DC. Tick marks on the circumference of the circle indicate the predicted values for the specified cylinder axes. The experimental results found on the model eye are depicted by the filled circles. The experimental results differ from the predicted values by less than 5° and 0.4 mm.

(2) The tilt of the crescent has to be measured with respect to the orientation of the knife edge (the orientation perpendicular to the camera–flash axis). A clockwise tilt in the range from 0° to 90° is associated with a positive sign. A counterclockwise tilt is associated with a negative sign (range: −0°–−90°).

(3) The above form of the inverse solution cannot be applied to astigmatic ametropias with or against the rule. In these situations both crescents have a tilt of 0°, resulting in undefined 0/0 division problems. In these conditions the basic Eqs. (2) and (3) should be used.

(4) Given a symmetric mixed astigmatism, both crescents are always of equal size but opposite sign, and both tilts are identical. In these conditions the cylinder angle α cannot be evaluated from Eq. (17) because both k_2 and k_4 are 0. However, in these conditions, α can be simply set to $\gamma/2$ if $DCR_h > 0$ and to $(180° + \gamma)/2$ if $DCR_h < 0$ (see Figs. 3 and 4).

(5) In all other cases we can avoid division-by-zero problems by replacing the denominator of k_3 with a small number.

7. VERIFICATION ON A MODEL EYE

In order to verify the results predicted by the theory, we used a photorefractor similar to Fig. 1. The photorefractor consisted of a 35-mm camera with a 150-mm lens and a halogen lamp mounted at an eccentricity of 11.8 mm below the horizontal borderline of an opaque mask that covered the lower half of the lens. The model eye consisted of an 80-mm achromatic lens and an adjustable, white painted metal plate modeling the retina. The pupil diameter was 16 mm. The model eye was adjusted to emmetropia.[20] A refractive deficit was introduced by the placement of trial lenses in front of the model eye. Pictures of the reflex from the fundus appearing in the pupil of the model eye were taken from a distance of 1 m. A series of pictures was taken at a number of mixed and simple astigmatic errors. For every combination of trial lenses, the axis was rotated through 180° in steps of 10°.

Figure 5 shows a comparison between experimentally obtained data points for a trial lens of 0.25 DS, −3.0 DC and the circle described by the crescent vector according to the theory. All measured values are in close agreement with the predicted values. In general, the tilt of the crescent differed by less than 3° from the values predicted by Eq. (13); the maximal deviation was 5°. The size of the dark crescent differed by less than 0.5 mm from the values specified by Eq. (12).

8. DISCUSSION

The foregoing analysis showed that the size and the tilt of the crescent can be predicted from five of the six parameters specified in Eq. (4). Equations (12) and (13) indicate that the dark crescent size and tilt is independent of pupil size. It has been emphasized in the literature[11,18,21] that care must be taken to measure the pupil size when one is estimating the refractive error with an eccentric photorefractor. This discrepancy arises from our use of the dark crescent measure, i.e., the size of the pupil not filled with light. Howland's original Eq. (10) for the dark fraction, *DF*,[18] can be rewritten in the present notation as

$$DF = DCR/2R_p = e/[2R_p(d_c D_{\text{sph}} - 1)].$$

It can be shown from this formula that the pupil size cancels out when the dark crescent size, *DCR*, instead of the dark fraction, *DF*, is used as the dependent variable and that it is only necessary to measure the distance between the pupil margin and the crescent border. However, as we mentioned in Section 3, pupil size is an important constraint on the sensitivity and accuracy of the method.

For the derivation presented in Appendix A, we assume that the two intersections, S_{c1} and S_{c2}, between the knife edge and the blur ellipse lie inside the aperture of the camera (see Fig. 10 below). This assumption may be violated (1) in the case of a large ametropia (large blur ellipse), (2) in the case of a simple astigmatism (the blur ellipse is constricted to a line that may not hit the EP at all), and (3) when the diameter of the camera aperture is small. In these cases the crescent size and tilt may differ from those in the theory, or the crescent border may have round edges or may be completely invisible. These limitations are especially pronounced in photorefractors that incorporate a small light source or a small observation aperture as, e.g., in the ingenious, simple point-spread retinoscope[21] with which the crescent is observed with the small EP of the human eye.

The effect of a limited EP was also observed in our model experiments. For example, we were not able to observe the crescent for some cylinder angles in the case of a simple astigmatism. With an ametropia of −1.0 DS, −3.0 DC and a camera distance of 1 m, the tilt of the crescent showed an orderly behavior for a cylinder axis of less than 60°: The tilt was always equal to the cylinder axis. At an axis of 60°, however, a discontinuous transition from an easily visible crescent to a totally dark pupil occurred.

The influence of a limited EP of the camera is illustrated in Fig. 6(a). An ametropia that creates a narrow

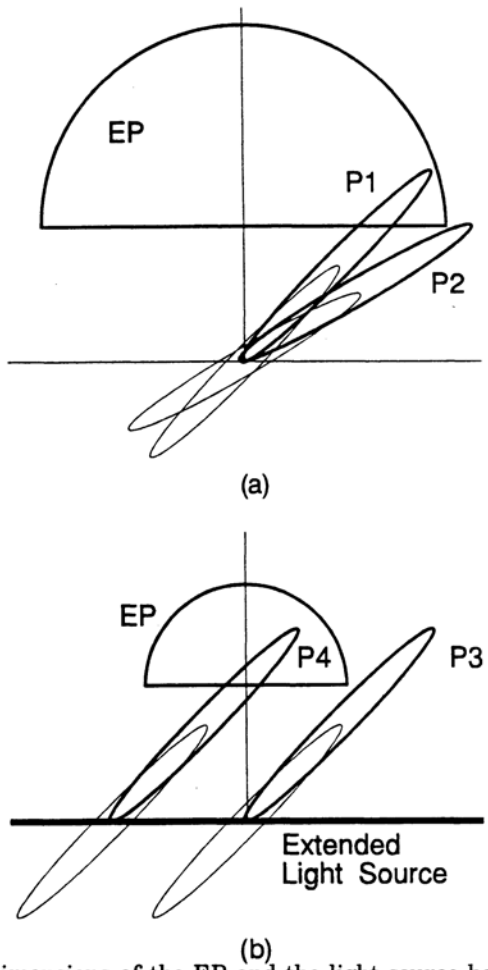

Fig. 6. Dimensions of the EP and the light source have an important influence on the detectability and the orderly behavior of the crescent (see text).

ellipse in the camera plane as shown in Fig. 6(a) will generate a crescent according to the theory when the ellipse is tilted as depicted in position P1. The same ametropia will not create a crescent at all when the ellipse is tilted as depicted in position P2 because the blur ellipse lies outside the camera EP.

The effect of a limited camera EP may be overcome in part with an extended linear light source orientated parallel to the knife edge instead of a point source. An extended flash tube consists of a large number of laterally displaced light sources that create laterally displaced blur ellipses. This setup enhances the ability to observe the crescent in the pupil. As illustrated in Fig. 6(b), the blur ellipse created by the centered light source, P3, does not hit the camera EP. However, a laterally displaced portion of the light source creates a displaced ellipse, P4, that will generate a regular crescent according to the theory presented above.

From the foregoing analysis it is clear that a single picture of the crescent cannot effectively be used to screen for astigmatic errors. In particular, astigmatisms with or against the rule give rise to a crescent with a horizontal border when a horizontally aligned camera is used, thus making the crescent indistinguishable from a crescent created by a purely spherical ametropia. More importantly, simple astigmatisms at an axis orthogonal to the orientation of the photorefractor are undetectable. However the foregoing analysis shows that two pictures are sufficient for determination of the spherical and cylindrical power of the ametropia, provided that both pictures show a measurable crescent.

The model experiment has shown that the theory can predict the size and the tilt of the crescent from the optical properties of the model eye. However, one should keep in mind that our model eye had a higher optical quality than a normal human eye (i.e., a high-quality lens, a large pupil, and a highly reflecting image plane). In a real screening situation for the human eye, one will encounter additional problems that are not covered by the geometric-optics approach described here. Among these problems are (1) ill-defined crescent borders owing to the shallow continuous transition at the edge of the crescent, (2) colored crescent borders owing to chromatic aberration, and (3) a scissor effect similar to streak retinoscopy, i.e., a visible crescent appears on opposite sides of the pupil in a single picture. However, the theoretical framework of photoretinoscopy presented here may serve as a guideline that helps to improve the accuracy of the existing designs.

APPENDIX A

In this appendix the size and the tilt of the dark crescent will be determined for an astigmatic eye with arbitrary cylinder axis. It will be shown that the size and the tilt of the crescent can be completely described in terms of the spherical and the cylindrical power, D_{sph} and D_{cyl}, the cylinder axis, α, the eccentricity of the flash, e, and the distance of the camera, d_c. Further variables in the course of the derivation are the pupil radius, R_p, and the distance of the retina from the nodal point, d_r. In order to simplify the derivation, we will use a coordinate system that rotates with the cylinder axis α (Fig. 1).

Step I: Dimensions of the Blur Ellipse on the Retina

An ametropic eye creates a blurred retinal image of the flash. First we determine the radii of the blur ellipse R_{rx} and R_{ry}.

Assuming an astigmatic ametropia of D_{sph} combined with D_{cyl} axis α at vertex distance 0, we can obtain the refractive power of the eye's optical system in the two principal meridians by subtracting the refractive error from the refractive power of an emmetropic eye, D_{eye}, that has the same length d_r as the eye under consideration ($D_{eye} = 1/d_r$). The resulting expressions for the refractive power in the two principal meridians D_x *and* D_y and the associated focal lengths f_x and f_y are

$$D_x = D_{eye} - D_{sph} = 1/f_x,$$
$$D_y = D_{eye} - D_{sph} - D_{cyl} = 1/f_y. \quad \text{(A1)}$$

The actual value of D_{eye} is unimportant. D_{eye} is set to $60D$ in the computations described below. Throughout the derivations f_x and f_y will be used instead of D_{sph} and D_{cyl}.

From the meridional focal length f_x or f_y, the positions of the meridional flash images b_x and b_y (Fig. 7) can

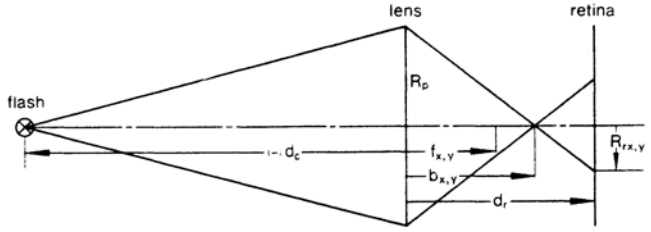

Fig. 7. Marginal rays define the radii of the blur ellipse on the retina, $R_{rx,y}$.

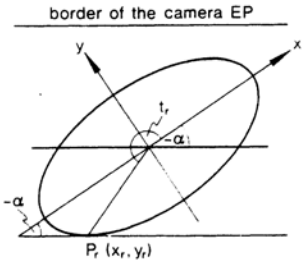

Fig. 8. Retina: the extreme point $P_r(x_r, y_r)$ on the tilted retinal blur ellipse is specified by a horizontal tangent.

be found:

$$b_{x,y} = (1/d_c + 1/f_{x,y})^{-1}, \tag{A2}$$

where the abbreviation $b_{x,y}$ stands for b_x and b_y when $f_{x,y}$ represents the meridional focal length f_x or f_y, respectively. This short-form notation, which enables one to write a single equation instead of two, will be used throughout this appendix.

The illuminating light rays diverge behind the meridional focal points (Fig. 7) and form a blur ellipse on the retina. The principal radii R_{rx} and R_{ry} of the ellipse are found from similar triangles as

$$R_{rx,y} = (b_{x,y} - d_r)R_p/b_{x,y}. \tag{A3}$$

Step II: Position of the Point on the Retinal Blur Ellipse That Appears Lowest on the Retina

In this important step of the derivation, we calculate the coordinates of the retinal point $P_r(x_r, y_r)$, which appears lowest on the retina. This point is solely responsible for the border of the crescent because it will be imaged highest in the plane of the camera (see P_c in Figs. 9 and 10 below). As is shown in Fig. 8, P_r is specified by

(1) a slope of the tangent of $-\alpha$ and

(2) $x_r, y_r < 0$ if $0° < \alpha < 90°$ or $x_r < 0$ and $y_r > 0$ if $90° < \alpha < 180°$.

The general form of the slope of the tangent to an ellipse in P_r is

$$\tan(-\alpha) = -x_r R_{ry}^2/y_r R_{rx}^2. \tag{A4}$$

After inserting x_r and y_r from the parametric form of the ellipse,

$$x_r = R_{rx}\cos(t_r), \tag{A5}$$

$$y_r = R_{ry}\sin(t_r), \tag{A6}$$

and elementary operations, we obtain the polar angle t_r of P_r as

$$t_r = \arctan\{R_{rx}/[R_{ry}\tan(\alpha)]\}. \tag{A7}$$

Observing the sign rule described above, we find that the coordinates of the extreme point P_r are given by

$$x_r = \text{sgn } x_1|R_{rx}\cos(t_r)|, \tag{A8}$$

$$y_r = \text{sgn } y_1|R_{ry}\sin(t_r)|, \tag{A9}$$

with sgn $x_1 = -1$, sgn $y_1 = -1$ if $0° < \alpha < 90°$ or sgn $y_1 = 1$ if $90° < \alpha < 180°$.

Step III: Position and Radii of the Blur Ellipse Generated in the Camera Plane by the Retinal Point $P_r(x_r, y_r)$

The light reflected off the fundus at P_r forms a blur ellipse in the camera plane. We determine the equation of this blur ellipse.

Each point inside the retinal blur ellipse gives rise to a conoid of Sturm in object space. The meridional focal lines are situated in the meridional far-point planes at distances of a_x and a_y from the eye (Fig. 9):

$$a_{x,y} = (1/d_r - 1/f_{x,y})^{-1} = (D_{\text{eye}} - D_{x,y})^{-1}. \tag{A10}$$

In the plane of the camera, the conoid of Sturm forms a blur ellipse with principal radii R_{cx} and R_{cy}. R_{cx} and R_{cy} can be easily obtained from similar triangles (Fig. 9):

$$R_{cx,y} = (a_{x,y} - d_c)R_p/a_{x,y}. \tag{A11}$$

The blur ellipse generated by the extreme retinal point P_r will be centered at an off-axis point $P_c(x_c, y_c)$ that is defined by the intersection between the chief ray through P_r (Fig. 8) and the camera plane. P_c has the coordinates

$$x_c = d_c x_r/d_r, \qquad y_c = d_c y_r/d_r. \tag{A12}$$

Thus the blur ellipse in the camera plane centered at P_c is described by

$$(x - x_c)^2/R_{cx}^2 + (y - y_c)^2/R_{cy}^2 = 1. \tag{A13}$$

Step IV: Intersection between the Blur Ellipse [Eq. (A13)] and the Border of the Entrance Pupil of the Camera

The blur ellipse in the camera plane centered at P_c may have intersections with the knife edge of the camera EP. The light rays passing above this borderline (hatched area in Fig. 10) enter the camera and form the bright crescent. Here we derive the coordinates of the intersections S_{c1} and S_{c2}.

Given an ametropia with cylinder axis α, the border of the EP is described in the rotated coordinate system by the basic formula

$$x\cos(\beta) + y\sin(\beta) - e = 0, \tag{A14}$$

where $\beta = 90° - \alpha$ is the angle between the x axis and the perpendicular to the border of the EP (Fig. 9). After a transformation to the normal form, we find that

$$y = mx + n, \tag{A15}$$

with

$$m = -\cos(\beta)/\sin(\beta),$$

$$n = e/\sin(\beta). \tag{A16}$$

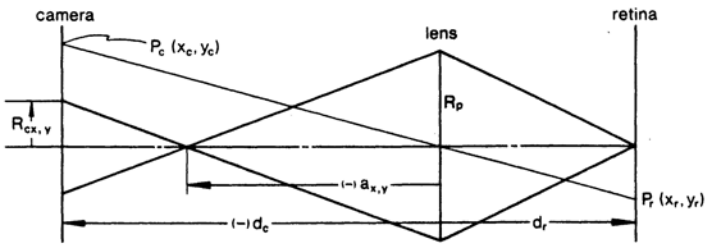

Fig. 9. Each point inside the retinal blur ellipse generates a blur ellipse with main radii $R_{cx,y}$ in the camera plane. The blur ellipse in the camera plane generated by P_r is centered at P_c.

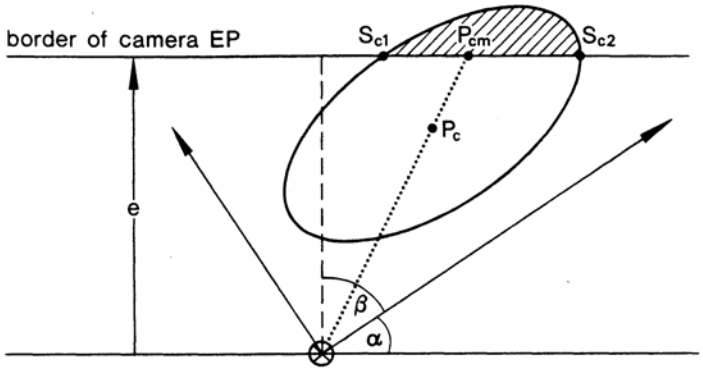

Fig. 10. Camera plane: the light rays of the blur ellipse passing inside the EP (hatched area) create the bright crescent. The dark crescent is greater than the pupil radius when P_c lies outside the EP.

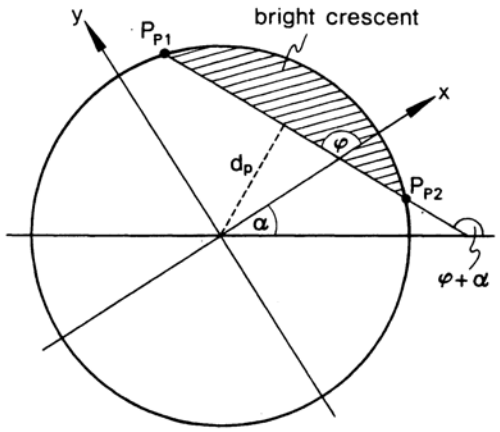

Fig. 11. Pupil plane: the two points P_1 and P_2 at the rim of the pupil that are associated with the intersections S_{c1} and S_{c2} in the camera plane (Fig. 10) define the border of the crescent.

The x and y coordinates of the two intersections S_{c1} and S_{c2} between the border of the EP [Eq. (A15)] and the blur ellipse centered at P_c [Eq. (A13)] are obtained after elementary calculations as

$$x_{s1,2} = -\frac{k}{2g} \pm \left(\frac{k^2}{4g^2} - \frac{h}{g}\right)^{1/2}, \tag{A17}$$

$$y_{s1,2} = mx + n, \tag{A18}$$

with

$$g = R_{cy}^2 + m^2 R_{cx}^2,$$

$$k = 2m(n - y_c)R_{cx}^2 - 2x_c R_{cy}^2,$$

$$h = x_c^2 R_{cy}^2 + (n - y_c)R_{cx}^2 - R_{cx}^2 R_{cy}^2.$$

No crescent appears when the square root from Eq. (A17) is negative (no intersection).

Step V: Identification of the Marginal Rays Generating the Crescent

The intersections S_{c1} and S_{c2} between the blur ellipse centered at P_c and the border of the EP [Eqs. (A17) and (A18)] define two marginal rays. These rays emerge in the retinal point P_r (Fig. 9) and pass the pupil at the two points P_{p1} and P_{p2} (Fig. 11). These two points at the rim of the pupil define the boundary of the crescent.

In order to understand how the coordinates of these two points can be determined, the reader should try to visualize the optical path of the light rays that create the blur ellipse depicted in Fig. 10. These light rays originate in the retinal point P_r (Fig. 9), pass through the circular pupil of the eye, and form a conoid of Sturm outside the eye. In every cross section the conoid of Sturm has an ellipsoid shape (including the two focal lines, the circular pupil, and the circle of least confusion as special cases of the ellipse).

From the laws of projective geometry, it can easily be shown that two given points on the boundary of the conoid of Sturm (e.g., S_{c1} and S_{c2} of Fig. 10) are associated with two conjugated points at the margin of the pupil (i.e., P_{p1} and P_{p2} of Fig. 11).

The coordinates of these two points at the margin of the pupil can be obtained mathematically by the transformation of the ellipse [Eq. (A13)] into a circle with pupil radius R_p centered at the origin.

Furthermore, one has to identify a possible sign change. A sign change occurs, e.g., in a meridian that is myopic with respect to the camera because the light rays are focused and cross one another in front of the camera (see Fig. 9):

$$\text{sgn } x_2 = -1 \quad \text{if} \quad (D_{\text{eye}} - 1/d_c) < D_x, \tag{A19}$$

$$\text{sgn } y_2 = -1 \quad \text{if} \quad (D_{\text{eye}} - 1/d_c) < D_y. \tag{A20}$$

Hence the coordinates in the pupil that define the boundary of the crescent are obtained as

$$x_{p1,2} = \text{sgn } x_2 |(x_{s1,2} - x_c)R_p/R_{cx}|, \tag{A21}$$

$$y_{p1,2} = \text{sgn } y_2 |(y_{s1,2} - y_c)R_p/R_{cy}|. \tag{A22}$$

Step VI: Size and Tilt of the Crescent

Finally, the tilt of the crescent with respect to the rotated coordinate system can be calculated from the slope of the line connecting the two boundary points $P_{p1,2}$, resulting in

$$\phi = \arctan[(y_{p2} - y_{p1})/(x_{p2} - x_{p1})]. \tag{A23}$$

The final value for the magnitude of the tilt in the normal horizontal coordinate system can be obtained by the addition of the cylinder axis α (see Fig. 11):

$$\gamma = \phi + \alpha. \tag{A24}$$

In order to determine the size of the dark crescent, we initially calculate the distance d_p of the secant $P_{p1}P_{p2}$ from the origin:

$$d_p = [(x_{p1} + x_{p2})^2/4 + (y_{p1} + y_{p2})^2/4]^{1/2}. \tag{A25}$$

The remaining problem to be solved is to determine whether d_p has to be added to or subtracted from the pupil radius so that we can obtain the size of the dark crescent (i.e., to decide whether the dark crescent is larger or smaller than the pupil radius). We can answer this question by considering the locus of the central point inside the blur ellipse, P_c, as illustrated in Fig. 10. When P_c lies outside the EP of the camera, the dark crescent, formed by the portion of the ellipse outside the EP, is larger than the portion of the ellipse inside the EP. This indicates that the dark crescent is larger than the pupil radius, and d_p has to be added to R_p. Mathematically, this problem can be solved by determining whether the point P_{cm} on the border of the EP in the direction of P_c has a larger distance from the origin than does P_c (Fig. 10). The distance

d_1 of P_c [Eq. (A12)] from the origin is

$$d_1 = (x_c^2 + y_c^2)^{1/2}. \quad \text{(A26)}$$

We can derive the coordinates of P_{cm} by calculating the intersection between the line that describes the border of the EP [Eq. (A14)] and the line connecting the origin and P_c, i.e., $y = (y_c/x_c)x$, resulting in

$$x_{cm} = e/[\cos(\beta) + (y_c/x_c)\sin(\beta)], \quad \text{(A27)}$$

$$y_{cm} = e/[\sin(\beta) + (x_c/y_c)\cos(\beta)]. \quad \text{(A28)}$$

From Eqs. (A27) and (A28), the distance d_2 of the boundary point P_{cm} from the origin in the direction of P_c is found as

$$d_2 = (x_{cm}^2 + y_{cm}^2)^{1/2}. \quad \text{(A29)}$$

Finally, the size of the dark crescent can be written as

$$DCR = R_p + \text{sgn}(d_2 - d_1)d_p. \quad \text{(A30)}$$

The distance d_p of the secant P_1P_2 from the origin has to be subtracted when the sign function $\text{sgn}(d_2 - d_1)$ is negative.

Equations (A24) and (A30) completely describe the size and the tilt of the dark crescent. In order to calculate these values, we need Eqs. (A1)–(A3), (A7)–(A12), and (A16)–(A29).

Numerical Evaluation

The results presented in Section 4 of this paper have been calculated on a microcomputer from analytical expressions with the use of double-precision variables. Problems arise in some special cases, e.g., when the cylinder angles are 180° or 90° and when f_x or f_y are equal to d_r. In the latter case the blur ellipse is contracted into a focal line. These problems occur because arguments in the denominator of some equations are 0 [see, e.g., Eq. (A10)]. In those cases the 0 in the denominator was replaced by a very small number (10^{-6}), a technique that yields a sufficiently accurate result.

ACKNOWLEDGMENTS

This research was carried out at the Smith–Kettlewell Eye Research Institute while W. Wesemann was supported by grant 1-F05-TW033830-01 from the Fogarty International Center, National Institutes of Health, Bethesda, Maryland. Further support was provided by grants EY 06883, EY 06579, and G 008635115. We thank the three anonymous reviewers for many valuable suggestions.

REFERENCES AND NOTES

1. H. Littmann, "Foveale Praezisionsskiaskopie," v. Graefe's Arch. Klin. Ophthalmol. **149,** 520–539 (1949).
2. H. C. Howland and B. Howland, "Photorefraction: a technique for study of refractive state at a distance," J. Opt. Soc. Am. **64,** 240–249 (1974).
3. H. C. Howland, O. J. Braddick, J. Atkinson, and B. Howland, "Optics of photorefraction: orthogonal and isotropic methods," J. Opt. Soc. Am. **73,** 1701–1708 (1983).
4. K. Kaakinen, "A simple method for screening of children with strabismus, anisometropia or ametropia by simultaneous photography of the corneal and fundus reflexes," Acta Ophthalmol. **57,** 161–171 (1979).
5. K. Kaakinen, "Simultaneous two flash static photoskiascopy," Acta Ophthalmol. **59,** 378–385 (1980).
6. K. Kaakinen, "Procedure and means for establishing and recording errors of the eye," U.S. patent 4,523,820 (June 18, 1985).
7. S. H. Hay, J. H. Kerr, R. R. Jayroe, J. C. White, and M. Funke, "Retinal reflex photometry as a screening device for amblyopia and pre-amblyopic states in children," South J. Med. **76,** 309–312 (1983).
8. S. H. Day and A. M. Norcia, "Photographic detection of amblyogenic factors," Ophthalmology **93,** 25–28 (1986).
9. A. M. Norcia, K. Zadnik, and S. H. Day, "Photorefraction with a catadioptric lens," Acta Ophthalmol. **64,** 379–385 (1986).
10. A. C. B. Molteno, J. Hoare-Nairne, J. C. Parr, I. J. Hodgkinson, N. E. O'Brien, and S. D. Watts, "The Otago photoscreener, a method for the mass screening of infants to detect squint and refractive errors," Trans. Ophthalmol. Soc. N. Z. **35,** 43–49 (1983).
11. W. R. Bobier and O. J. Braddick, "Eccentric photorefraction: optical analysis and empirical measures," Am. J. Optom. Physiol. Opt. **62,** 614–620 (1985).
12. F. Schaeffel, L. Farkas, and H. C. Howland, "Infrared photoretinoscope," Appl. Opt. **26,** 1505–1509 (1987).
13. M. R. Angi and A. Cocchiglia, "Il videorefrattometro binoculare infrarosso: uno strumento per lo screening dei difetti ambliogenici e lo studio dinamico della capacita accomodativa," Boll. Oculist. **69,** Suppl. 4, 305–320 (1990).
14. F. Schaeffel and H. C. Howland, "Properties of the feedback loops controlling eye growth and refractive state in the chicken," Vision Res. **31,** 717–734 (1991).
15. W. H. A. Fincham and M. H. Freeman, *Optics*, 9th ed. (Butterworth, London, 1980), p. 420. The term knife-edge principle originally describes a single-pass geometry. Refraction techniques based on Foucault's knife-edge test use a double-pass geometry. The light source and the knife edge are mounted in the same plane. The retina serves as a reflecting surface.
16. H. C. Howland, "The optics of static photographic skiascopy," Acta Ophthalmol. **58,** 221–227 (1980).
17. C. W. Tyler and A. M. Norcia, "Ray-tracing analysis of the optics of paraxial photorefraction," in *Noninvasive Assessment of Visual Function,* Vol. 6 of 1985 OSA Technical Digest Series (Optical Society of America, Washington, D.C., 1985), pp. WA3-1–WA3-4.
18. H. C. Howland, "The optics of photoretinoscopy: results from ray tracing," Am. J. Optom. Physiol. Opt. **62,** 621–625 (1985).
19. Figure 1 of the paper of Bobier and Braddick[11] plots a ray diagram that shows the crescent formation of a myopic eye. Their drawing is not fully correct because a retinal point A, located above the optical axis, is imaged to a point A′, which is also located above the optical axis. This is not possible since an object A and a real image A′ always lie on opposite sides of the optical axis.
20. In order to adjust the model eye to emmetropia, we replaced the model retina by a front surface mirror. The light of a He–Ne laser was imaged into the eye. The position of the mirror was altered until the reflected light ermerged parallel (autocollimation technique). Finally, the diffusely reflecting model retina was inserted at exactly the same position as the mirror.
21. H. C. Howland, N. Sayles, C. Cacciotti, and M. Howland, "Simple pointspread retinoscope suitable for visual screening," Am. J. Optom. Physiol. Opt. **64,** 114–122 (1987).